International Journal of Innovative Computing, Information and Control
Volume **18**, Number **4**, August **2022**

ICIC International ©2022 ISSN 1349-4198
pp. **1071–1088**

ANALYSIS OF THE THROUGHPUT OF THE PRODUCTION SYSTEM WITH THE AID OF GENERAL RELATIVITY

Kenji Shirai[1], Yoshinori Amano[2], Atsuya Ando[1] and Takayuki Uda[1]

[1]Faculty of Business and Informatics
Niigata University of International and Information Studies
3-1-1, Mizukino, Nishi-ku, Niigata 950-2292, Japan
dr.kenji5761@gmail.com; { atsuya; uda }@nuis.ac.jp

[2]Kyohnan Elecs Co., LTD.
8-48-2, Fukakusanishiura-cho, Fushimi-ku, Kyoto 612-0029, Japan
y_amano@kyohnan-elecs.co.jp

Received January 2022; revised April 2022

Abstract. *This paper analyzes the superiority of a synchronic production system based on the general theory of relativity. The statistical parameters that significantly influence flow are the mean value and volatility. In the application of relativity, mass is introduced as a parameter derived from mean and volatility. That mass is the value of the production system. We chose Riemannian space as a suitable space for calculating this mass. A method for improving throughput is presented by considering the polar coordinate system in Riemannian space. Generally, in relativity theory, the speed of light is invariant; however in the production system, the goal is the target point. The velocity of light on the theory of relativity is the volume of production in a production system. The final conclusion is that it is possible to exceed the intended production volume by altering the conditions of the production system. Additionally, a numeric example is presented as a specific example. Generally, in relativity theory, the speed of light is invariant; however in the production system, the goal is the target point, and if the requirements of the production system are changed, we can say that is not impossible.*

Keywords: Throughput, Production process, General theory of relativity, Minkowski space, Tensor analysis

1. **Introduction.** The authors have reported mathematical modeling of production processes, estimation of the production status of each process, optimal control problems, and flow analysis in small and medium scale [1, 2, 3, 4, 5, 6]. We have constructed the state in which the production density of each process corresponds to the physical propagation of heat [2, 7]. Using this approach, we have shown that the diffusion equation dominates the manufacturing process. In other words, when minimizing the potential of the production field (stochastic field), the equation, which is defined by the production density function $S_i(x,t)$ and the boundary conditions, is described using the diffusion equation with advection to move in transportation speed ρ. The boundary conditions mean the closed system in the production field. The adiabatic state in thermodynamics represents the same state [2, 7].

Regarding with the optimal production capacity, we have reported that the quantity produced is proportional to the rate of return, which aids corporate development and limits production capacity. Therefore, we have employed the Hamilton-Jacobi-Bellman equation to calculate optimal production capacity and determine optimal parameters of the quadratic form evaluation function based on the optimal production capacity [8].

DOI: 10.24507/ijicic.18.04.1071

Then, we have investigated a method for optimal control of production processes that include lead-time delays. We have proposed the model that expresses lead-time lag in a strict mathematical model and the model with lead-time delay based on the average regression process, which is the Ornstein-Uhlenbeck process model that is used in mathematical finance. Optimal control is obtained using each state equation [9]. Also, the previous research applying Fluid mechanics that the trial production of a new concept vertical take-off and landing rotorcraft of flexible kite wing attached multicopter is very interesting [10].

Regarding with the throughput model for a production flow system, we have introduced the Riemannian manifold, which is easier to implement than stochastic modeling methods [4, 5]. This model is derived from the stochastic throughput model for producing the propagation necessary to measure synchronization. We have also introduced the Fisher information matrix to specify volatility. To validate the new method and clarify the synchronization processes, we perform a dynamic simulation of the production system. We have also presented the real synchronous and asynchronous data obtained from the production flow process. No other research has introduced Riemann manifold to demonstrate the superiority of synchronous production systems. Furthermore, we have clarified that the geometric structure of the production space, which consists of production steps and workers, should be described. Then the discussion went on about the production space like the Riemannian space.

We present the superiority of a synchronic production system based on the general theory of relativity. The mean value is the productivity trend, and one of the volatilities is the interest rate for government bonds in the economy, that is, the safe interest rate. These statistical parameters allow to calculate the throughput. In the application of relativity, the center of mass is introduced as a parameter derived from the mean value and volatility. Therefore, the central mass is defined within the Riemann space, and the outcome of the analysis in the throughput improvement is reported using the mass tensor. We regard the quantum field as equivalent to a production field, and the probability distribution of the throughput of a production field with an arbitrary region is assumed to have zero potential in the Schrodinger equation. We got a normal distribution around the original. If this is the case, the polar coordinates are constructed at an arbitrary point (σ: volatility) by rotating it at an angle around the origin. To conclude, in the one-dimensional space-time of Minkowski in the production system, the production volume increases linearly with the throughput. Usually, in the theory of relativity, the speed of light is invariant, but in a production system, the throughput corresponding to the speed of light is variable. The target point that depends on that throughput can be modified by changing the conditions of the production system. Most previous studies analyze the production process as a static model. We have the advantage of systematically dealing with the production process as a dynamic model and analyzing throughput and other factors. The reason is that the real process can be analyzed taking account of temporal and spatial fluctuation factors. Furthermore, there is no literature on the flow analysis of production processes that introduces the general theory of relativity.

The flow of the entire paper is as follows.

- We have traditionally expressed a mathematical model of throughput in a production process in a Euclidean coordinate system. Throughput is defined by time, mean and volatility.
- Originally, the throughput of a product in a production field can be considered as the value of a production system. We define a mass derived from throughput estimated

from the mean and volatility. This mass is analyzed for throughput improvement using a polar coordinate system in Riemannian space.

- We introduce the idea of general relativity as an analysis of improved performance. In conclusion, we present that the speed of light in the general theory of relativity can be improved for the entire production process by matching it to the maximum throughput in the production field.

2. Production Business of a Small-to-Midsize Firm.

2.1. Production systems in the production equipment industry.

We refer to the production system in manufacturing equipment industry studied in this paper. This is not a special system, but "Make-to-order system with version control". Make-to-order system is a system which allows necessary manufacturing after taking orders from clients, resulting in "volatility" according to its delivery date and lead time. In addition, "volatility" occurs in lead time depending on the contents of make-to-order products (production equipment). However, effective utilization of the production forecast information on the orders may suppress certain amount of "variation", but the complete suppression of variation will be difficult. In other words, "volatility" in monthly cash flow occurs and of course influences a rate of return in these companies. Production management systems, suitable for the separate make-to-order system which is managed by numbers assigned to each product upon order, is called as "product number management system" and is widely used. All productions are controlled with numbered products and instructions are given for each numbered product.

Thus, ordering design, logistics and suppliers are conducted for each manufacturer's serial numbers in most cases except for semifinished products (unit incorporated into the final product) and strategic stocks. Therefore, careful management of the lead time or production date may not suppress "volatility" in manufacturing (production). The company in this study is the "supplier" in Figure 1 and "factory" here. In Figure 1(A), the "Customer side" refers to an ordering company and "Supplier (D)" means the target company in this paper. The product manufacturer, which is the source of the ordered production equipment, presents an order that takes account of the market price. In Figure 1(B), the market development department at the customer's factory receives the order through the sale contract based on the predetermined strategy.

This is the data actually measured by the order side (Client) and the order side (Supplier to be researched) shown in Figure 1. It presents the production process data that received an order for a particular customer out of several existing customers. The client is a major semiconductor manufacturer. We have a long history of producing equipment.

2.2. Production flow system.

A manufacturing process that is termed as a production flow process is shown in Figure 2. The production flow process, which manufactures low volumes of a wide variety of products, is produced through several stages in the production process. In Figure 2, the processes consist of six stages. In each step S1-S6 of the manufacturing process, materials are being produced by one worker of each step S1 through S6. S1-S6, which are given by Tables 2, 4, 6 and 8 in Appendix A, correspond to the process in Figure 2. The throughput will vary greatly depending on the proficiency level of the worker (Testrun1 through Testrun3-2 in Appendix A).

The direction of the arrow represents the direction of the production flow. In this system, production materials are supplied from the inlet and the end product will be shipped from the outlet.

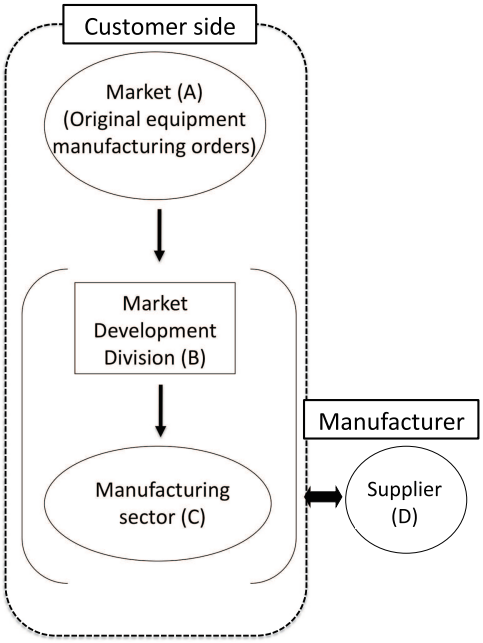

FIGURE 1. Business structure of company of research target

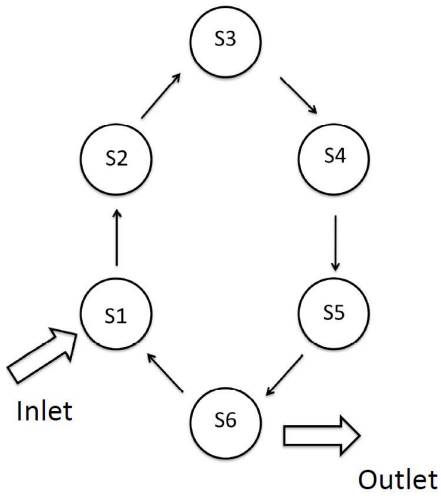

FIGURE 2. Production flow process

Assumption 2.1. *The production structure is nonlinear.*

Assumption 2.2. *The production structure is a closed structure; that is, the production is driven by a cyclic system (production flow system).*

- Reasonability of Assumption 2.1. Assumption 2.1 indicates that the determination of the production structure is considered a major factor, which includes the generation value of production or the rate of return generation structure in a stochastic manufacturing process (hereafter called the manufacturing field). Because such a structure is at least dependent on the demand, it is considered to have a nonlinear structure. Because the value of such a product depends on the rate of return, its production structure is nonlinear. Therefore, Assumption 2.1 reflects the realistic production structure and is somewhat valid.
- Reasonability of Assumption 2.2. Assumption 2.2 is completed in each step and flows from the next step until stage S6 is completed. Assumption 2.2 is reasonable because new production starts from S1. A more detailed analysis, please refer to our Appendix A.

3. Mathematical Model of Throughput Going through the Production Process.

3.1. **Mathematical model of the production system in the Euclid space.** In the Euclid coordinate system, the throughput $S^*(t, \mu, r_o)$ is defined by the following equation [11].

Definition 3.1.

$$\frac{1}{2}r_o^2\frac{\partial S^*}{\partial \mu^2} + mS^*\frac{\partial S^*}{\partial \mu} + \frac{\partial S^*}{\partial t} - r_o S^* = 0 \tag{1}$$

where μ, r_o and m are the average throughput of production system, the volatility of the entire process and the revenue variable respectively.

At this time, the throughput $S^*(t, \mu, r_o)$ is derived from the mean value and volatility estimated from the mass (value) of the original production system. In addition, μ and r_o can be considered as statistical parameters as throughput in $S^*(t, \mu, r_o)$. The boundary condition of $S^*(t, \mu, r_o)$ is given by the following equation.

$$S^*(\mu_H, r_o) = \frac{K}{r_o}\mu_H, \quad S^*(\mu_L, r_o) = 0 \tag{2}$$

where $\mu_L \leqq \mu \leqq \mu_H$.

From Figure 3, the following equation is obtained through the formulation of the continuous evaluation [5].

$$S^* = E\Big[(1 - r_o dt)\{S^* + dS^*\} + d\theta | \mathcal{F}^\theta\Big] \tag{3}$$

As described above, the production density function in the origin production field is given as a stochastic system by the following equation [5].

$$\partial S(t, x) = \mathcal{L}_x S(t, x)\partial t + r(t, x)\partial W(t, x) \tag{4}$$

where $\mathcal{L}_x$ is Laplace-Beltrami operator [4, 5].

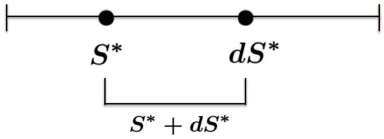

FIGURE 3. Continuous evaluation of production system

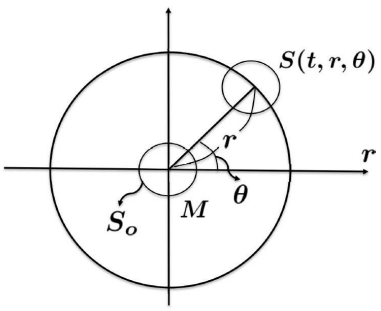

FIGURE 4. Centre mass tensor $S(t, r, \theta)$ in Riemannian space

At this time, μ and r exist as statistical parameters obtained from $S(t, x)$. The derivative function $S^*(t, \mu, r_o)$ can be computed using these estimates. From this, Equation (2) can be derived as a continuous equation for the production field, and Equation (1) can be calculated. Furthermore, the boundary condition Equation (5) can be defined by the constraint condition of $\mu_L \leqq \mu \leqq \mu_H$. So the following equation is defined as the mass of the production field.

Definition 3.2. *Centre mass M of the production field*

$$M = \rho(r_o)m, \quad \rho(r_o) = \frac{K\mu_H}{r_o}, \quad K > 1,\ 0 < m \leqq 1 \tag{5}$$

The centre mass M of the production field can be calculated using Equation (5). Besides, since the operator $\mathcal{L}_x$ of Equation (4) is originally defined on the Riemannian space, the Riemannian space is suitable as the space of the production field. For this reason, we consider the following simple model to be the system of coordinates of the production field.

3.2. **A simple model of a production system based on the general theory of relativity.** Here, the centre mass tensor $S(t, r, \theta)$ is given by the following equation [12].

$$S(t, r, \theta) = S^r_\theta d\mu_r d\mu^\theta \tag{6}$$

At that time, according to Figure 4, the model of the production system in the Riemannian space is considered in the system of polar coordinates.

$$m = (1+\beta), \quad 0 \leqq \beta \leqq 1, \quad M = \rho(r_o)m, \quad \rho(r_o) = \frac{S_o}{r_o} \tag{7}$$

$$r_S = \frac{2G\rho(r_o)m}{h_C^2} = \frac{2GS_o/r_o \cdot (1+\beta)}{h_C^2} = \frac{2GS_o(1+\beta)}{h_C^2 r_o} \tag{8}$$

The variables in Equations (7) and (8) are as follows:

- S_o: Production mass (relative cost)
- $\rho(r_o)$: Production density
- m: Production efficiency coefficient
- r_o: Entire production field
- r_S: Spatial distance of production field
- h_C: In general relativity, it has to do with the speed of light. In the production field, it represents the throughput (production speed) that cannot be exceeded, and it is assumed that h_C exists.

The mass potential at the center of Figure 5 is given by the following equation.

$$h_\phi = -G\frac{M}{r} \tag{9}$$

where r is the spatial distance of production field.

In Figure 6, the difference between A, B and C equals the difference of frequency k.

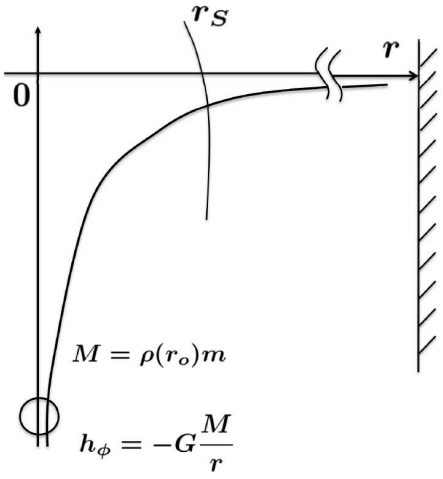

FIGURE 5. Central mass (value) potential

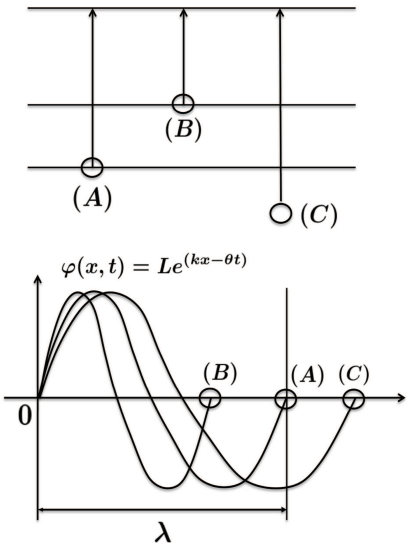

FIGURE 6. Volatility from synchronization point (phase)

In Figure 4, r, θ, and t have the following meanings, respectively.

- $S(t, r, \theta)$: Production tensor
- r: Deviation from the synchronization point (distance)
- θ: Deviation from synchronization point (phase)
- t: Deviation from synchronization point $\propto h$

The Riemannian metric is thus given by the following equation according to the general theory of relativity.

$$dS^2 = g_{o\theta} dr d\theta \tag{10}$$

where $g_{o\theta}$ is called a metric tensor. This metric tension defines the distance and determines the nature of the space.

If we put the metric tensor Equation (10) as the following equation, the Riemannian metric dS is given by the following equation [13].

$$dS^2 = -e^{\nu(r)}dt^2 + e^{\lambda(r)}dr^2 + r^2 d\theta^2 \tag{11}$$

where $e^{\nu(r)}$ and $e^{\lambda(r)}$ are the functions to simplify differentiation and integration calculations.

Between S and N in Figure 7, the curved surface is curved along the spherical surface. Therefore, the distance is different between (A) and (B). That is going to be different from the distance in the Cartesian coordinate system. $h(x)$ is given by the following equation.

$$h(x) \cong \frac{1}{\sqrt{2\pi}} \exp\left\{-\frac{1}{2}\left(\frac{x}{2\pi}\right)^2\right\} = \frac{1}{\sqrt{2\pi}} \exp\left\{-\frac{1}{2}\xi^2\right\} \tag{12}$$
$$\xi = \frac{x}{2\pi}, \quad \xi = (-a, +a), \quad a > 0$$

As described above, it is considered equivalent to the productive field in the quantum field. It is assumed that the probability distribution of the throughput of the production field with an arbitrary region has zero potential in the Schrodinger equation. Under this assumption, if you have a standard normal distribution around the origin, you can form a polar coordinate system at an arbitrary point (volatility r) by rotating it at an angular velocity around the origin. Therefore, if the production tensor on polar coordinates is set to S, it can be defined as $S = S(t, r, \theta)$ in Figure 8. Therefore, if the potential at the origin is set at h_ϕ, the following equation can be defined.

Definition 3.3. *Potential h_ϕ at the origin*

$$h_\phi = -\frac{G\rho(r_o)m}{r} \tag{13}$$

From Figure 4, the central production mass is the synchronous mass, and $M \ggg 0$. Figure 9 shows the mass production transition in Schwarzschild's space-time. The

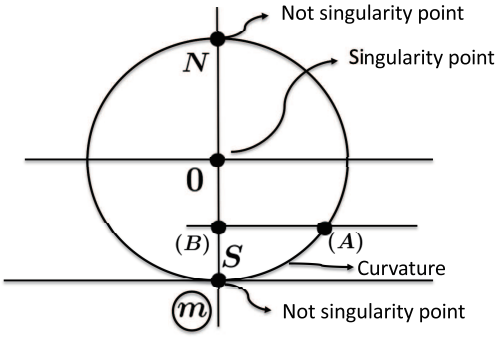

FIGURE 7. Spherical coordinate system

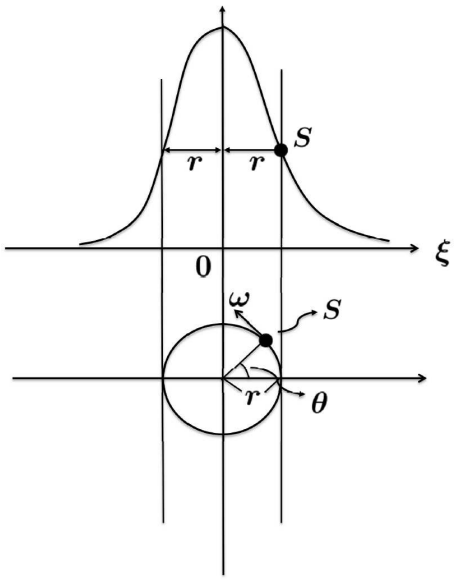

FIGURE 8. Probability density function of throughput and $S(t, r, \theta)$ polar coordinate system

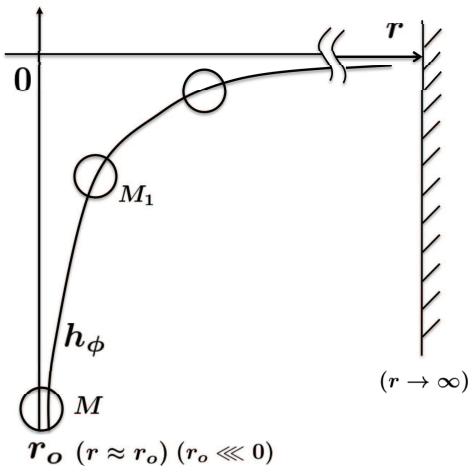

FIGURE 9. Mass production transition in Schwarzschild's space-time

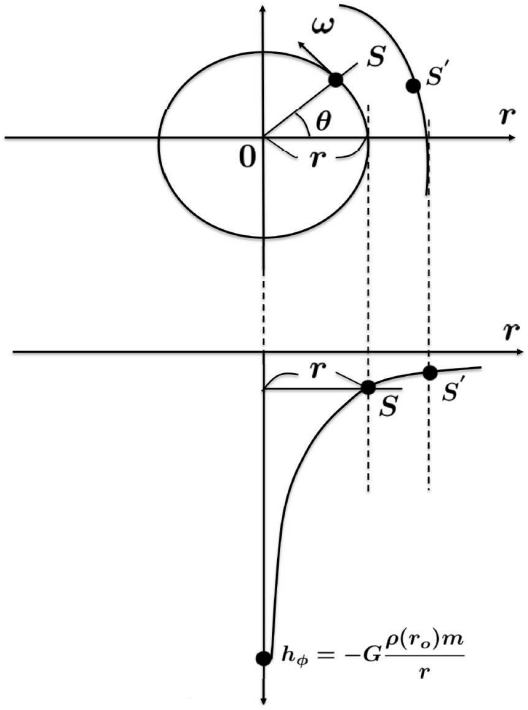

FIGURE 10. Potential h_ϕ in polar coordinate system

Schwarzschild metric dS^2 in spherically symmetric coordinates are given by [14]

$$dS^2 = -\left(1 - \frac{2GM}{h_C^2 r}\right) dt^2 + \left(1 - \frac{2GM}{h_C^2 r}\right)^{-1} dr^2 + r^2 d\theta^2 \tag{14}$$

For example, if $\theta = \frac{\pi}{2}$ is fixed, the following equation is obtained from Figure 10.

$$dS^2 = -\left(1 - \frac{2G\rho(r_o)m}{h_C^2 r}\right) dt^2 + \left(1 - \frac{2G\rho(r_o)m}{h_C^2 r}\right)^{-1} dr^2 + r^2 d\theta^2 \tag{15}$$

In Figure 11, the unique frequency ($\propto r$) of the system decreases as the production system changes to the synchronization point (r_o). In Figures 10 and 12, a signal starts from the source of the measurement at the production point (S) and goes to the synchronization point (r_o). Upon observation on S, it is delayed by u ($= t - r^*$).

4. **Numerical Example of Production System.** The numbers presented below are the numbers used in the production flow system in Appendix A and the numbers we think are reasonable in developing the logic. Figure 13 shows the major functions. The points (a), (b), and (c) in Figure 13 are analyzed.

$$h(\xi) = \frac{1}{\sqrt{2\pi}} \exp\left(-\frac{\xi^2}{2}\right), \quad \xi \in [\alpha, \beta] \tag{16}$$

$$M = \rho(r)m, \quad \rho(r) = \frac{M_D}{M_S}, \quad 0 < m \leqq 1 \tag{17}$$

The point (a) represents an asynchronous singularity. The meaning of each variable is as follows.

- $\rho(r_o)$: Mass density (asynchronous point)
- m: Coefficient of production effectiveness (subjective constant)

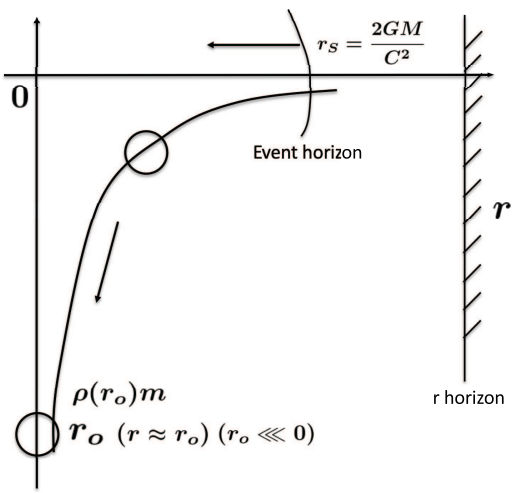

FIGURE 11. Situation approaching point of synchronization

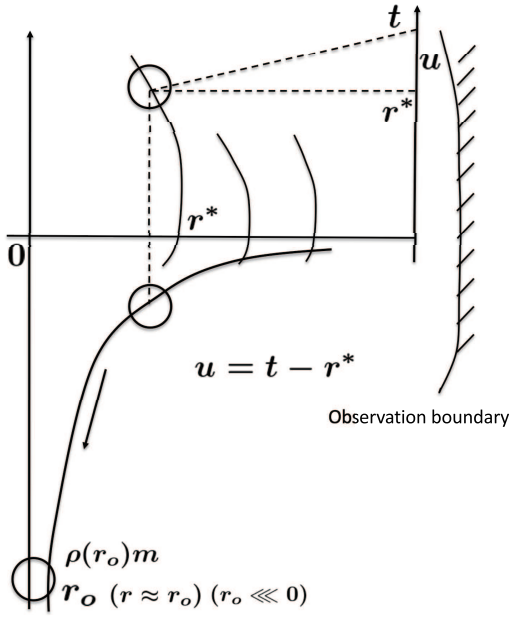

FIGURE 12. Transition to synchronization point

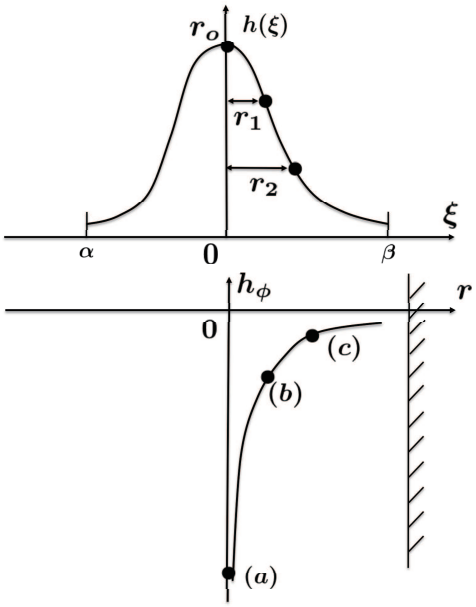

FIGURE 13. Production mass in polar coordinate system

- M_R: Lead time after improvement of production system
- M_o: Lead time before improvement of production system

Here, assuming the asynchronous point mass M, the mass potential h_ϕ is given in the following equation.

$$h_\phi = -G\frac{\rho(r_o)m}{r_o} = -G\frac{M}{r_o}, \quad \rho(r_o) = r_o^{-1}S_o, \quad G \equiv Constant \tag{18}$$

$$M \equiv \rho(r_o)m, \quad 0 < m \leqq 1, \quad m = \frac{M_R}{M_o}, \quad M_R < M_o \tag{19}$$

where r_o is not null and is of small value. For example, $r = 0.1$, that is, it was established on the assumption that there would not be a contradiction in logic. Further, m is process improvement coefficient, and $0 < m \leqq 1$. Moreover, S_o is the inherent mass of the production system assumed, and when normalized, it is assumed that it takes the values $0 < S_o \leqq M$. Therefore, $\rho(r_o)$ is given by the following equation.

$$\rho(r_o) = r_o^{-1} S_o = \frac{1}{r_o} S_o = \frac{54}{0.1} \times 1.0 = 540, \quad S_o = 54 \tag{20}$$

As well, $m = 1.0$ is the maximum value in terms of r_o. Therefore, M is given in this equation.

$$M = \rho(r_o) m = 540 \times 1.0 = 540 \tag{21}$$

$$r_S = \frac{2G\rho(r_o)}{h_C^2} = \frac{2 \times 10^{-1} \times 540 \times 1}{h_C^2} = \frac{108}{36} = 3.0, \quad G = 1.0 \times 10^{-1},\ 0 < m \leqq 1 \tag{22}$$

Normally, the volatility r_o is $0 < r_o \leqq 1$, when standardized, but in the vicinity of the singularity r_o, if $r_o = 0.1$, it is calculated as $1/r_o = 10$. In other words, the production system fell apart. The aforementioned variables have the following meanings:

- $h_C = 6$: Maximum production target (6 equipment) per day for the production flow system in Appendix A
- $S_o = 54$: Lead time for all production flow systems (Testrun1, Testrun2, Testrun3-1 and Testrun3-2) in Appendix A
- $\rho(r_o) = \frac{S_o}{r_o}$: Value near the singularity ($r_o = 0.1$)
- $G = 1.0 \times 10^{-1}$: Potential conversion factor
- $m = \frac{M_R}{M_o}$: Process improvement coefficient ($0 < m \leqq 1$) from the logic

where $h_C = Constant$ in the calculation. M_R is the maximum production volume (5.5) presented in Appendix A. M_o is the target production volume (6). The M_R was calculated to be 5.4 for simplicity. Therefore, m is 0.9. r_o was set from the logic of $0 < r_o \leqq 1$.

A specific numerical example is given. Assuming that $M_R = 54$ and $M_o = 60$ are the respective values, the following calculation results are achieved.

- $m = \frac{54}{60} = 0.9$
- $h_C = 6$
- $r_S = \frac{2 \times 10^{-1} \times 600 \times 0.9}{6^2} = \frac{108}{36}$
- $\sigma_S = \frac{36}{108} = 0.33$: $r_S = \frac{1}{\sigma_S}$

Here, since $S_o = M_R$ is set, the following value is obtained.

$$\rho(r_o) = \frac{M_R}{r_o}, \quad m = \frac{M_R}{M_o} \quad \Rightarrow \quad r_S = \frac{2G\rho(r_o)m^{-1}}{h_C^2} = \frac{2G\rho(r_o)}{h_C^2 \cdot m} = \frac{2G\rho(r_o)}{h_C^2 \left(\frac{M_R}{M_o}\right)} \tag{23}$$

Therefore, σ_S is given the following equation.

$$\sigma_S = \left[\frac{2G\rho(r_o)}{h_C^2 \left(\frac{M_R}{M_o}\right)} \right]^{-1} \tag{24}$$

According to the definition of production mass as described above, when the synchronous intrinsic mass tends to increase, if the process improvement is performed, the r_S asynchronization boundary parameter can be calculated based on the improvement process. This means improving performance through process improvement. However, specific examples of process improvement are not specified here.

5. **Synchronous Production Model in Minkowski Space.** The production system is a flat space-time consisting of synchronous mass and not affected by the potential. However, in the case of a production system, $C \equiv h_C$. However, C and h_C are the speed of light and the maximum number of production equipment. The metric tensor is given by the following equation.

$$dS^2 = -h_C^2 dt^2 + dx^2 + dy^2, \quad (h_C t, x, y) \equiv (0, 0, 0) \tag{25}$$

Figure 14 shows the following.

- $\sqrt{x^2 + y^2} = h_C t$: Progress status at light velocity.
- $\sqrt{x^2 + y^2} < h_C t$: It can be achieved more slowly than light. In this case, it cannot coexist with the origin. Therefore, only time is prioritized.
- $\sqrt{x^2 + y^2} > h_C t$: It takes more than light's speed to get there. In this case, it cannot be reached. Therefore, only space is prioritized.

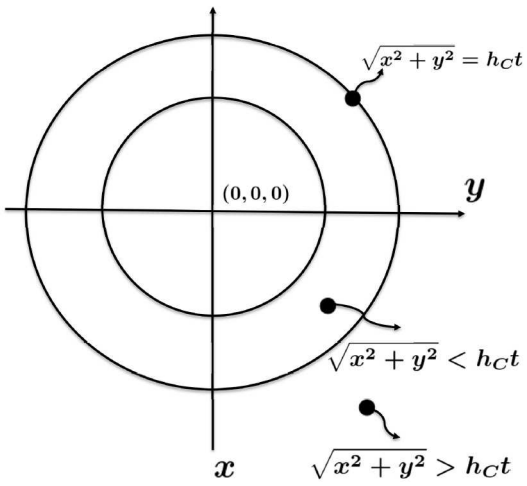

FIGURE 14. Production system operating zone

We analyze in more detail in the one-dimensional case.

$$h_C^2 dt^2 = dx^2, \quad \Rrightarrow \quad h_C = \sqrt{\left(\frac{dx}{dt}\right)^2} = \frac{dx}{dt} \tag{26}$$

In view of the fact that the x process is almost equal to the specific mass $S(x)$ of the process, the following equation is applied.

$$h_C \equiv \frac{\partial S(x)}{\partial t}, \quad \partial S(x) = S(x_1) - S(x_2) \tag{27}$$

That is, h_C returns to the definition of normal throughput. That is, in the Minkowski space-time in the production system, the amount of production increases linearly according to the throughput h_C.

- (A): $h_C t > x$; $t > T_o$ – Do not share the initial value (0). Here, the time asynchronous area is shown.
- (B): $h_C t < x$; $t < T_o$ – The initial value (0) is shared, but can only be achieved if $h_C^{'} > h_C$ appears.
- (C): $h_C t = x$; $t = T_o$ – Synchronous area.

Figure 16 shows the arrival status at the coordinate point (T_o, x_{T_o}) in one-dimensional Minkowski time. Point (A) is the case of $h_C t > x$, and the initial value is not shared by Figure 16 to reach as time increases. That is, the arrival condition is $t > T_o$. Point

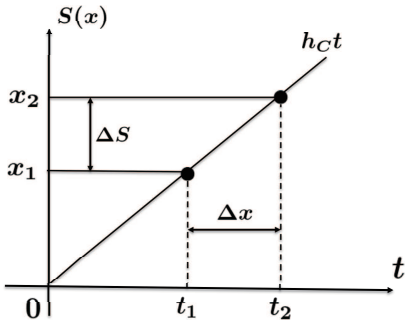

FIGURE 15. Dealing with the specific mass $S(x)$

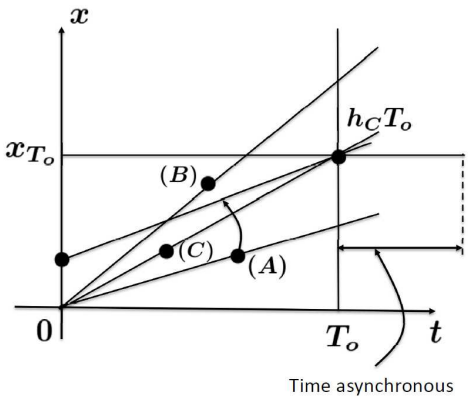

FIGURE 16. One-dimensional Minkowski space-time

(B) is the case of $h_C t < x$, which does not achieve, but shares the initial value (0). That is, $t < T_o$ when the above condition is fulfilled. Point (C) is the case of $h_C t = x$, which is one point in Minkowski space-time. At this time, $t = T_o$. Therefore, the area (A) is called a time domain (time asynchronous), the area (B) is called a spatial area (spatial asynchronous), and the area (C) is called a space-time matching area (synchronous area). Naturally, in (A) and (B), the volatility r for T_o is $r > 0$, and in (C), $r = 0$.

6. **Conclusion.** By defining the production mass, it was found that if the synchronous eigenmas increase, the process improvement can be performed to calculate the asynchronous boundary parameters according to the improvement process. This means improving performance by improving the process. Generally, the speed of light is invariant in the theory of relativity, but in the production system, the target is the target point, and it is not impossible even if the requirements of the production system change.

As a next step in this paper, we start by expressing the throughput in the production field using tensor analysis. Finally, we demonstrate that by reducing production mass M, the area of the production field where synchronization is performed increases.

REFERENCES

[1] K. Shirai, Y. Amano and T. Uda, Manufacture allocation of the batch process and the cyclic flow process via stochastic analysis, *International Journal of Innovative Computing, Information and Control*, vol.16, no.3, pp.939-954, 2020.

[2] K. Shirai, Y. Amano and A. Ando, Analytical mechanics approach to conservation in production field, *International Journal of Innovative Computing, Information and Control*, vol.17, no.1, pp.67-91, 2021.

[3] K. Shirai, Y. Amano and T. Uda, Cost reduction function considering stochastic risks in the production process, *International Journal of Innovative Computing, Information and Control*, vol.16, no.4, pp.1257-1278, 2020.

[4] K. Shirai and Y. Amano, Use of a Riemannian manifold to improve the throughput of a production flow system, *International Journal of Innovative Computing, Information and Control*, vol.12, no.4, pp.1073-1087, 2016.

[5] K. Shirai, Y. Amano, A. Ando and T. Uda, Spatial properties of production flow system based on Riemannian manifold structure, *International Journal of Innovative Computing, Information and Control*, vol.17, no.3, pp.831-851, 2021.

[6] K. Shirai, Y. Amano, A. Ando and T. Uda, Evaluation of production flow system utilizing expected high volume effective rate, *International Journal of Innovative Computing, Information and Control*, vol.17, no.4, pp.1203-1224, 2021.

[7] H. Tasaki, *Thermodynamics – A Contemporary Perspective (New Physics Series)*, Baifukan Co., LTD., 2000.

[8] K. Shirai and Y. Amano, An optimal production capacity control including outside suppliers, *International Journal of Innovative Computing, Information and Control*, vol.13, no.1, pp.167-182, 2017.
[9] K. Shirai and Y. Amano, Optimal control of production processes that include lead-time delays, *International Journal of Innovative Computing, Information and Control*, vol.15, no.1, pp.21-37, 2019.
[10] K. Hayama and H. Irie, Trial production of kite wing attached multicopter for power saving and long flight, *ICIC Express Letters, Part B: Applications*, vol.10, no.5, pp.405-412, 2019.
[11] K. Shirai and Y. Amano, Production throughput evaluation using the Vasicek model, *International Journal of Innovative Computing, Information and Control*, vol.11, no.1, pp.1-17, 2015.
[12] R. d'Inverno, *Introducing Einstein's Relativity*, Clarendon Press, 1992.
[13] M. Toda, *30 Lectures on Theory of Relativity (30 Lectures on Physics Series)*, Asakura Co., LTD., 1997.
[14] K. Sato, *Theory of Relativity*, Iwanami Co., LTD., 1996.

Appendix A: Analysis of Actual Data in the Production Flow System. Based on the control equipment, the product can be manufactured in one cycle. The rate of return required to maintain 6 pieces of equipment/day is as follows.

- (Testrun1): Because the throughput of each process (S1-S6) is asynchronous, the overall process throughput is asynchronous. In Table 1, we list the manufacturing time (min) of each process. In Table 3, we list the volatility in each process performed by the workers. Finally, Table 2 lists the target times. The theoretical throughput is obtained as $3 \times 199 + 2 \times 15 = 627$ (min). In addition, the total working time in stage S3 is 199 (min), which causes a bottleneck. In Figure 17, we plot the measurement data listed in Table 2, which represents the total working time of each worker (K1-K9). In Figure 18, we plot the data contained in Table 2, which represents the volatility of the working times.

Table 1. Correspondence between the table labels and the Testrun number

	Table number	Production process	Working time	Volatility
Testrun1	Table 2	Asynchronous process	627 (min)	0.29
Testrun2	Table 4	Synchronous process	500 (min)	0.06
Testrun3-1	Table 6	"Synchronization with preprocess" method	470 (min)	0.03
Testrun3-2	Table 8	"Synchronization with preprocess" method	470 (min)	0.03

Table 2. Testrun1

	WS	S1	S2	S3	S4	S5	S6
K1	15	20	20	25	20	20	20
K2	20	22	21	22	21	19	20
K3	10	20	26	25	22	22	26
K4	20	17	15	19	18	16	18
K5	15	15	20	18	16	15	15
K6	15	15	15	15	15	15	15
K7	15	20	20	30	20	21	20
K8	20	29	33	30	29	32	33
K9	15	14	14	15	14	14	14
Total	145	172	184	199	175	174	181

Table 3. Volatility of Table 2

	S1	S2	S3	S4	S5	S6
K1	1.67	1.67	3.33	1.67	1.67	1.67
K2	2.33	2	2.33	2	1.33	1.67
K3	1.67	3.67	3.33	2.33	2.33	3.67
K4	0.67	0	1.33	1	0.33	1
K5	0	1.67	1	0.33	0	0
K6	0	0	0	0	0	0
K7	1.67	1.67	5	1.67	2	1.67
K8	4.67	6	5	4.67	5.67	6
K9	0.33	0.33	0	0.33	0.33	0.33

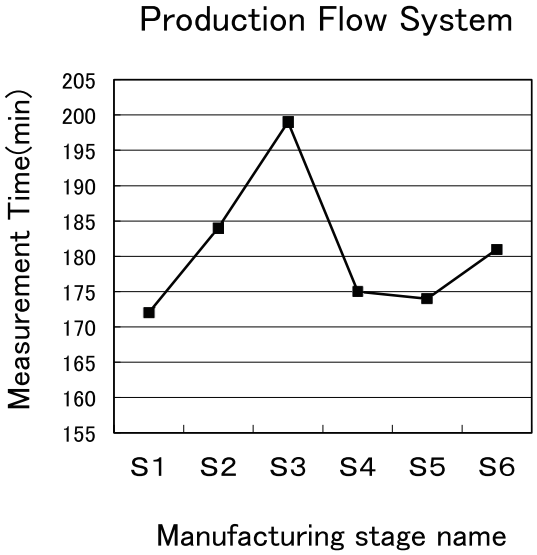

FIGURE 17. Total work time for each stage (S1-S6) in Table 2

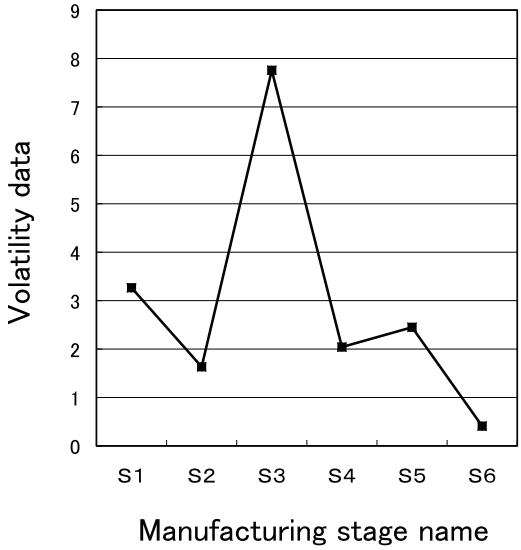

FIGURE 18. Volatility data for each stage (S1-S6) in Table 2

- (Testrun2): Set to synchronously process the throughput. The target time listed in Table 4 is 500 (min), and the theoretical throughput (not including the synchronization idle time) is 400 (min). Table 5 presents the volatility of each working process (S1-S6) for each worker (K1-K9).

TABLE 4. Testrun2

	WS	S1	S2	S3	S4	S5	S6
K1	20	20	24	20	20	20	20
K2	20	20	20	20	20	22	20
K3	20	20	20	20	20	20	20
K4	20	25	25	20	20	20	20
K5	20	20	20	20	20	20	20
K6	20	20	20	20	20	20	20
K7	20	20	20	20	20	20	20
K8	20	27	27	22	23	20	20
K9	20	20	20	20	20	20	20
Total	180	192	196	182	183	182	180

TABLE 5. Volatility of Table 4

	S1	S2	S3	S4	S5	S6
K1	0	1.33	0	0	0	0
K2	0	0	0	0	0.67	0
K3	0	0	0	0	0	0
K4	1.67	1.67	0	0	0	0
K5	0	0	0	0	0	0
K6	0	0	0	0	0	0
K7	0	0	0	0	0	0
K8	2.33	2.33	0.67	1	0	0
K9	0	0	0	0	0	0

- (Testrun3-1): Introducing a preprocess stage. The process throughput is performed synchronously with the reclassification of the process. As shown in Table 6, the theoretical throughput (not including the synchronization idle time) is 400 (min). Table 7 presents the volatility of each working process (S1-S6) for each worker (K1-K9).
- (Testrun3-2): same as Testrun3-1.

On the basis of these results, the idle time must be set to 100 (min). Moreover, the theoretical target throughput $\left(T_s'\right)$ can be obtained using the "Synchronization with preprocess" method. This goal is as follows:

$$\begin{aligned} T_s \sim\ & 20 \times 6 \text{ (First cycle)} + 17 \times 6 \text{ (Second cycle)} \\ & +20 \times 6 \text{ (Third cycle)} + 20 \text{ (Previous process)} + 8 \text{ (Idol-time)} \\ \sim\ & 370 \text{ (min)} \end{aligned} \tag{28}$$

Table 6. Testrun3-1

	WS	S1	S2	S3	S4	S5	S6
K1	20	18	19	18	18	18	18
K2	20	18	18	18	18	18	18
K3	20	21	21	21	21	21	21
K4	16	13	11	11	13	13	13
K5	16	16	16	17	17	16	16
K6	16	18	18	18	18	18	18
K7	20	14	14	13	14	14	13
K8	20	22	22	22	22	22	22
K9	20	25	25	25	25	25	25
Total	168	165	164	163	166	165	164

Table 7. Volatility of Table 6, K5: Preprocess

	S1	S2	S3	S4	S5	S6
K1	0.67	0.33	0.67	0.67	0.67	0.67
K2	0.67	0.67	0.67	0.67	0.67	0.67
K3	0.33	0.33	0.33	0.33	0.33	0.33
K4	1	1.67	1.67	1	1	1
K5	0	0	0.33	0.33	0	0
K6	0.67	0.67	0.67	0.67	0.67	0.67
K7	2	2	2.33	2	2	2.33
K8	0.67	0.67	0.67	0.67	0.67	0.67
K9	1.67	1.67	1.67	1.67	1.67	1.67

The full synchronous throughput in one stage (20 (min)) is

$$T_s^{'} = 3 \times 120 + 40 = 400 \text{ (min)} \tag{29}$$

Using the "Synchronization with preprocess" method, the throughput is reduced by approximately 10%. Therefore, we showed that our proposed "Synchronization with preprocess" method is realistic and can be applied in flow production systems. Below, we represent for a description of the "Synchronization with preprocess".

Table 8. Testrun3-2, K5: Previous process

	WS	S1	S2	S3	S4	S5	S6
K1	20	18	19	18	18	18	18
K2	20	18	18	18	18	18	18
K3	20	21	21	21	21	21	21
K4	16	13	11	11	13	13	13
K5	*	*	*	*	*	*	*
K6	16	18	18	18	18	18	18
K7	16	14	14	13	14	14	13
K8	20	22	22	22	22	22	22
K9	20	20	20	20	20	20	20
Total	148	144	143	141	144	144	143

Table 9. Volatility of Table 8, K5: Previous process

	S1	S2	S3	S4	S5	S6
K1	0.67	0.33	0.67	0.67	0.67	0.67
K2	0.67	0.67	0.67	0.67	0.67	0.67
K3	0.33	0.33	0.33	0.33	0.33	0.33
K4	1	1.67	1.67	1	1	1
K5	*	*	*	*	*	*
K6	0.67	0.67	0.67	0.67	0.67	0.67
K7	0.67	0.67	1	0.67	0.67	1
K8	0.67	0.67	0.67	0.67	0.67	0.67
K9	0	0	0	0	0	0

In Table 8, the working times of the workers K4, K7 show shorter than others. However, the working time shows around target time. Next, we manufactured one piece of equipment in three cycles. To maintain a throughput of six units/day, the production throughput must be as follows:

$$\frac{(60 \times 8 - 28)}{3} \times \frac{1}{6} \simeq 25 \text{ (min)} \tag{30}$$

where the throughput of the preprocess is set to 20 (min). In Equation (30), the value 28 represents the throughput of the preprocess plus the idle time for synchronization. Similarly, the number of processes is 8 and the total number of processes is 9 (8 plus the preprocess). The value of 60 is obtained as 20 (min) $\times$ 3 (cycles).

In Table 1, Testrun3-1/Testrun3-2 indicate a best value for the throughput in the three types of theoretical working time. Testrun2 is ideal production method. However, because it is difficult for talented worker, Testrun3-1/Testrun3-2 are a realistic method.

In Table 6 and Table 8, Testrun3-1/Testrun3-2 indicate a best value for the throughput in the three types of theoretical working time. Testrun2 is ideal production method. However, because it is difficult for talented worker, Testrun3-1/Testrun3-2 are a realistic method.

The results are as follows. Here, the trend coefficient, which is the actual number of pieces of equipment/the target number of equipment, represents a factor that indicates the degree of the number of pieces of manufacturing equipment.
Testrun1: 4.4 (pieces of equipment)/6 (pieces of equipment) = 0.73,
Testrun2: 5.5 (pieces of equipment)/6 (pieces of equipment) = 0.92,
Testrun3-1 and Testrun3-2: 5.7 (pieces of equipment)/6 (pieces of equipment) = 0.95.
Volatility data represent the mean value of each Testrun.

Appendix B: Table to Summarize Figures and Formulas in this Paper.

TABLE 10. Title of figures

Figure number	Title name of figure No.
Figure 1	Business structure of company of research target
Figure 2	Production flow process
Figure 3	Continuous evaluation of production system
Figure 4	Centre mass tensor $S(t, r, \theta)$ in Riemannian space
Figure 5	Central mass (value) potential
Figure 6	Volatility from synchronization point (phase)
Figure 7	Spherical coordinate system
Figure 8	Probability density function of throughput and $S(t, r, \theta)$ polar coordinate system
Figure 9	Mass production transition in Schwarzschild's space-time
Figure 10	Potential h_ϕ in polar coordinate system
Figure 11	Situation approaching point of synchronization
Figure 12	Transition to synchronization point
Figure 13	Production mass in polar coordinate system
Figure 14	Production system operating zone
Figure 15	Dealing with the specific mass $S(x)$
Figure 16	One-dimensional Minkowski space-time
Figure 17	Total work time for each stage (S1-S6) in Table 2
Figure 18	Volatility data for each stages (S1-S6) in Table 2

TABLE 11. Title of notations

Notation number	Title name of notation No.
Equation (1)	Mathematical model of production process throughput $S^*(t, \mu, r_o)$
Equation (2)	Boundary condition of $S^*(t, \mu, r_o)$
Equation (3)	Continuous evaluation equation
Equation (4)	Production density function in the origin production field
Equation (5)	Centre mass M of the production field
Equation (6)	Centre mass tensor $S(t, r, \theta)$
Equation (7)	Production efficiency coefficient
Equation (8)	Spatial distance of production field
Equation (9)	Mass potential at the center of Figure 5
Equation (10)	Riemannian metric according to the general theory of relativity
Equation (11)	Riemannian metric dS for simplifinng differentiation and integration calculations
Equation (12)	Curved surface distance between (A) and (B) in Figure 7
Equation (13)	Potential h_ϕ at the origin
Equation (14)	Schwarzschild metric dS^2 in spherically symmetric coordinates
Equation (15)	Schwarzschild metric dS^2 in spherically symmetric coordinates in case of $\theta = \frac{\pi}{2}$
Equation (16)	Mass potential in Figure 13
Equation (17)	The centre mass M of the production field in Figure 13
Equation (18)	Mass potential h_ϕ in Figure 13
Equation (19)	Centre mass M and coefficient of production effectiveness (subjective constant) m
Equation (20)	Production density $\rho(r_o)$
Equation (21)	Centre mass M
Equation (22)	Spatial distance r_S of production field
Equation (23)	Spatial distance r_S of production field
Equation (24)	Inverse value $\rho(r_o)$ of r_S
Equation (25)	Metric tensor dS^2 in case of $C \equiv h_C$
Equation (26)	Formulation of h_C in the one-dimensional case
Equation (27)	Representation of h_C by specific mass $S(x)$ of the process
Equation (28)	Theoretical target throughput $\left(T_s^{'}\right)$
Equation (29)	Full synchronous throughput in one stage (20 min)
Equation (30)	Production throughput to maintain a throughput of six units/day

Author Biography

Kenji Shirai received the B.Sc. degree in Electrical Engineering from Ritsumeikan University, Japan, 1973; the M.Sc. degree in Electrical Engineering from Ritsumeikan University, Japan, 1975; the Ph.D. degree in Electrical Engineering from Ritsumeikan University, Japan, 2000.

Dr. Shirai is engaged in research on optimal control of distributed parameter systems, modeling of industrial systems applying mathematical finance, and optimal control.

Yoshinori Amano received the B.Sc. degree in Electrical Engineering from Ritsumeikan University, Japan, 1971; the M.Sc. degree in Electrical Engineering from Ritsumeikan University, Japan, 1973; the Ph.D. degree in Electrical Engineering from Ritsumeikan University, Japan, 1977.

Dr. Amano is engaged in research on optimal control of distributed parameter systems, modeling of information systems applying mathematical finance, and optimal control. Currently, he is Advisor of Kyohnan Electric Co., LTD.

Atsuya Ando received the Dr. Eng. degree in System Information Engineering from Tsukuba University, in 2013. In 1990, he joined the Nippon Telegraph and Telephone Corporation (NTT) Wireless Systems Laboratories, Yokosuka, Japan. He was engaged in research and development of personal and base station antennas for wireless mobile communication systems. From 2000 to 2003, he was with the ATR Adaptive Communications Research Laboratories, Kyoto, Japan, engaging in research and development on adaptive array antennas for wireless ad-hoc network systems. In 2019, he moved to Niigata University of International and Information Studies, and he is currently a Professor in the Department of Information Systems. His research interests include mobile and base station antennas using metamaterials for wireless communication systems.

Takayuki Uda received a doctoral degree (Information Science) from the Graduate School of Information Sciences, Tohoku University, Japan, in 2009; a master's degree (Informatics) from the University of Library and Information Science (now Information and Media Studies, University of Tsukuba).

Prof. Takayuki Uda is currently a full-time professor at the Department of Information Systems, Faculty of Business and Informatics, Niigata University of International and Information Studies. His research fields are data science and natural language processing. His research results contribute to the education and research of students.